

Nuclear Technology

ISSN: 0029-5450 (Print) 1943-7471 (Online) Journal homepage: http://www.tandfonline.com/loi/unct20

Long-Term Leaching Experiments of Full-Scale Cemented Waste Forms: Experiments and Modeling

Bernhard Kienzler, Peter Vejmelka, Horst-Jürgen Herbert, Herbert Meyer & Corinna Altenhein-Haese

To cite this article: Bernhard Kienzler, Peter Vejmelka, Horst-Jürgen Herbert, Herbert Meyer & Corinna Altenhein-Haese (2000) Long-Term Leaching Experiments of Full-Scale Cemented Waste Forms: Experiments and Modeling, Nuclear Technology, 129:1, 101-118, DOI: 10.13182/NT00-A3049

To link to this article: http://dx.doi.org/10.13182/NT00-A3049

Published online: 13 May 2017.

Submit your article to this journal

Article views: 1

View related articles

Citing articles: 2 View citing articles

Full Terms & Conditions of access and use can be found at
http://www.tandfonline.com/action/journalInformation?journalCode=unct20

Download by: [the LANL Research Library] **Date:** 16 November 2017, At: 15:19

LONG-TERM LEACHING EXPERIMENTS OF FULL-SCALE CEMENTED WASTE FORMS: EXPERIMENTS AND MODELING

RADIOACTIVE WASTE MANAGEMENT AND DISPOSAL

KEYWORDS: *cement, leaching, modeling*

BERNHARD KIENZLER* and PETER VEJMELKA
Forschungszentrum Karlsruhe, Institut für Nukleare Entsorgungstechnik (INE)
P.O. Box 3640, D-76021, Karlsruhe, Germany

HORST-JÜRGEN HERBERT *Gesellschaft für Anlagen- und Reaktorsicherheit mbH*
Bereich Endlagersicherheitsforschung, Braunschweig, Germany

HERBERT MEYER *GSF-Forschungszentrum für Umwelt und Gesundheit GmbH*
Forschungsbergwerk Asse, Germany

CORINNA ALTENHEIN-HAESE *Freie Universität Berlin*
Institut für Anorganische und Analytische Chemie, Berlin, Germany

Received November 17, 1998
Accepted for Publication June 30, 1999

Downloaded by [the LANL Research Library] at 15:19 16 November 2017

Experimental findings of full-scale leach tests performed on simulated cemented waste forms and self-shielded concrete waste containers for periods up to 19 yr in saturated salt brines (NaCl- and Q-brine) are presented. Measurements cover the evolution of leachant composition and the release of radionuclides such as Cs, U, and Np. Performance of the waste forms and the self-shielded concrete waste containers depends on the pore volume of the hardened cement/concrete, which is correlated to the water/cement ratio of the waste forms. Cesium release follows a linear time dependence. Samples, especially those having a high pore volume, show almost complete release of Cs in the period of investigation. Uranium release is independent of the leach period. Uranium concentrations are controlled by thermodynamic equilibrium. Neptunium is released only to a small extent; concentrations are close to the detection limit.

Modeling of the cement corrosion progress allows the prediction of the evolution of the brines in terms of pH, calcium concentration, etc. and the identification of solids controlling the solubilities of the main components and of uranium.

I. INTRODUCTION

Between 1990 and 1998 ~20 000 m^3 of low-level radioactive wastes (LLWs) were disposed of in the Morsleben repository in Germany (ERAM). These wastes hold 7.1×10^{10} Bq alpha activity and 7.1×10^{13} Bq beta/gamma activity.[1] The wastes originate from the operation of nuclear power plants, decommissioning, and applications of radionuclides in research, industry, and medicine. Cemented waste forms represent a significant part of the inventory of ERAM. Also, many of the ~120 000 containers of LLW disposed of during operation of the Asse salt mine as a research disposal site until 1978 contain cemented waste forms. Additionally, cement is brought into the repositories by self-shielding concrete containers or by construction materials for sealing and backfilling.

The associated risk of the disposal system depends on the mobilization of radioactive elements in the case of groundwater (brine) intrusion into the repository. In the case of a brine penetration into a repository, cement-based materials show a large capacity for changing the composition and pH of the brines. In a repository in rock salt such as Gorleben, ERAM, or the Asse research mine, highly concentrated salt brines may interact with the waste forms or with other cementitious materials. The

*E-mail: kienzler@ine.fzk.de

Downloaded by [the LANL Research Library] at 15:19 16 November 2017

interactions will result in dissolution of certain cement phases and precipitation of mineral phases and, consequently, in changes of the solution composition. Furthermore, the solution chemistry influences the solubility of radionuclides, e.g., by increasing the pH. Radionuclide release from the waste forms, radionuclide solubility, formation of solid phases (precipitation), migration, sorption, and colloid formation depend on the geochemical environment and its evolution.

Long-term safety analyses of nuclear waste repositories require reliable tools and databases for predictive modeling of radionuclide behavior. Many codes and databases are available for geochemical modeling. However, performance assessment calculations require extrapolations of short-term observations to time periods relevant for the isolation of long-lived radioactive waste.[2,3] To ensure a reliable prediction of the long-term radionuclide behavior, comparisons between the results of models and experiments are required. Models should cover the relevant physicochemical phenomena and include the pertinent thermodynamic and kinetic data, whereas experiments should be performed in such a way that the mechanisms underlying the models can be evaluated.

In the past, numerous experiments have been performed for the investigation of radionuclide release from cemented waste forms. Most of these experiments were performed for relatively short time periods and often nonequilibrium states were considered. Leaching was generally acknowledged to be the basic criterion for evaluating the quality of the conditioning (treatment and/or solidification) of radioactive wastes. Pore structure, leaching and corrosion behavior, radionuclide retention and other properties of cemented waste forms can be influenced by the fabrication process. To investigate the scale-up and to determine the influence of the technical cementation process on the properties of the cemented waste forms, full-scale leaching tests were started between 1978 and 1989. Different specimens were used in these leaching tests. In the former Kernforschungszentrum Karlsruhe (KfK),[a] simulated and real cemented waste forms were applied. In the Asse research mine simulated waste blocks up to 160 ℓ containing tracers such as ^{137}Cs, natural uranium, and ^{237}Np, respectively, were investigated in leach experiments. These experiments continue today. At the Commissariat à l'Energie Atomique in France, leaching experiments on 200-ℓ monoliths, consisting of liquid and solid wastes containing alpha, beta, and gamma emitters, embedded in cement or bitumen were performed.

Few long-term, full-scale experimental data on the performance of cemented waste forms and their release of radioactivity in brines are reported in the literature.[4–13] In this paper, the results of long-term experiments performed with full-scale samples in the FZK and in the Asse research mine are presented, and the findings are compared with geochemical modeling results.

II. EXPERIMENTAL

Inactive simulated cemented waste samples, typical for cemented intermediate-level wastes (ILW), were fabricated. The waste concentrates correspond to those originating from the reprocessing of spent fuel by the Purex process. The composition and properties of the concentrates are given in Ref. 12. The most abundant component of the concentrates was sodium nitrate. The cement products were prepared in such a way that the resulting waste form had a load of ~10 wt% of salts. Different techniques for mixing cement powder with simulated ILW concentrates were applied. The water/cement ratio (W/C) varied from 0.24 to 0.32, 0.45, and 0.5 in the samples, similar to that of real waste forms, ranging between 0.45 and 0.63. The unhydrated product was filled into drums having volumes between 85 and 200 ℓ. After complete hydration of the product, the drums were removed and the samples immersed into 400-ℓ containers filled with the corroding media. The characteristics of the different tests are listed in Table I. Tap water, NaCl-brine, and Q-brine were applied as leachants. The compositions of the corroding media are listed in Table II. Q-brine and NaCl-brine cover the most significant range of brine compositions, which may arise from the presence of different salt minerals in German salt domes. The samples at KfK were stored at 40°C, and those at the Asse mine were exposed to the ambient temperature at the 490-m level of 28 ± 1°C.

The waste forms used in the KfK experiments were produced in a manner similar to the industrial process of waste concentrate solidification with ordinary portland cement (OPC) Type PZ45, by application of in-drum mixers at the KfK cementing facility.[14] The Asse samples were produced in a way comparable to that at different facilities. Volumes of leachates amounted to 225 dm^3 per 160 dm^3 of sample at KfK and ranged from 250 dm^3 per 80-dm^3 sample to 124 dm^3 per 160-dm^3 specimen at Asse. The canisters were closed by lids equipped with sampling systems. In some cases, a loss of water could be observed after some years, and brine was added periodically. The loss of water may have been caused by an incomplete sealing system of the canisters. The corrosive media were not changed during the experimental period. Because of the construction of the lid-seal systems and the repeated sampling procedures, aerobic conditions have to be assumed.

Sampling was done periodically, at a high frequency during the initial period and only once a year after a few years of reaction. In KfK experiments, the corroding medium was mixed, whereas at Asse, most of the solutions remained undisturbed over long periods. In the Asse

[a] Now Forschungszentrum Karlsruhe (FZK).

TABLE I

Characteristics of Different Full-Scale Tests

	Type	Tracer	W/C Ratio	Leachant	Total Number of Samples	Sample Identification	Duration
KfK	Inactive	Cs	0.45	Q-brine	2	KfK 5 KfK 6	10.9 yr
	VBA[a]	– – –		Q-brine	1	VBA 1 VBA 2	11.7 yr
Asse	Inactive	– – –	0.24	Tap water	2	1, 6	Since 1979
	Inactive	Cs	0.24		2	13, 14	Since 1979
	Inactive	Cs	0.24	NaCl-brine	3	10, 11, 12	Since 1979
	Tracer	^{137}Cs	0.32		1	23	Since 1981
	Tracer	^{137}Cs	0.43		1	30	Since 1984
	Inactive	– – –	0.29	Q-brine	1	4	Since 1979
	Inactive	Cs	0.24		3	7, 8, 9	Since 1979
	Inactive	Cs	0.32		1	20	Since 1980
	Tracer	^{137}Cs	0.32		3	21, 22, 24	Since 1981
	Tracer	^{137}Cs	0.43		2	28, 29	Since 1984
	Tracer	U_{nat}	0.43	NaCl-brine	1	27	Since 1984
			0.50		2	31, 32	Since 1988
	Tracer	U_{nat}	0.30, 0.34	Q-brine	2	25, 26	Since 1984
		U inventory: 1kg/sample	0.50		2	33, 34	Since 1989
	Tracer	^{237}Np	0.50	NaCl-brine	1	35	Since 1989
	Tracer	^{237}Np	0.50	Q-brine	1	36	Since 1989

[a]VBA is a self-shielded concrete waste container having a wall thickness of ~20 cm, into which a standard 200-ℓ steel drum was inserted. This drum was filled with simulated cemented waste (PZ 45 HZ) having a load of 9.6 wt% of mainly $NaNO_3$ salt with 1.23 wt% of inactive Cs added as tracer. The gap between the drum and container and the lid was filled from the top with cement grout. The total mass of this VBA was 2.7 Mg.

TABLE II

Initial Leachant Compositions of the Full-Scale Experiments*

	Cl^- (mol/kg)	SO_4^{2-} (mol/kg)	Mg^{2+} (mol/kg)	Ca^{2+} (mol/kg)	Na^+ (mol/kg)	K^+ (mol/kg)	pH	Ionic Strength
Q-brine	8.67	0.29	4.08	1.4×10^{-4}	0.38	0.71	6.0	13.6
NaCl-brine	6.10	0.005	0.04	2.5×10^{-2}	6.10	0.038	7.0	6.3

*Concentrations in mol/kg H_2O.

experiments, it was possible to obtain samples from different vertical levels of the corroding media. Only in a few cases were the solutions mixed prior to sampling.

At Asse, determination of ^{137}Cs was done by means of an NaI well detector with a detection limit of 0.33 Bq/ml. Determination of inactive Cs was accomplished by atomic absorption spectroscopy. Uranium was measured by different methods, e.g., by photometric methods and by mass spectrometry (ICP-MS[b]). Measurements of inactive components of the solutions at FZK were performed by means of the ICP-AES[c] method.

[b]Inductively coupled mass spectrometry.
[c]Inductively coupled atomic emission spectroscopy.

Downloaded by [the LANL Research Library] at 15:19 16 November 2017

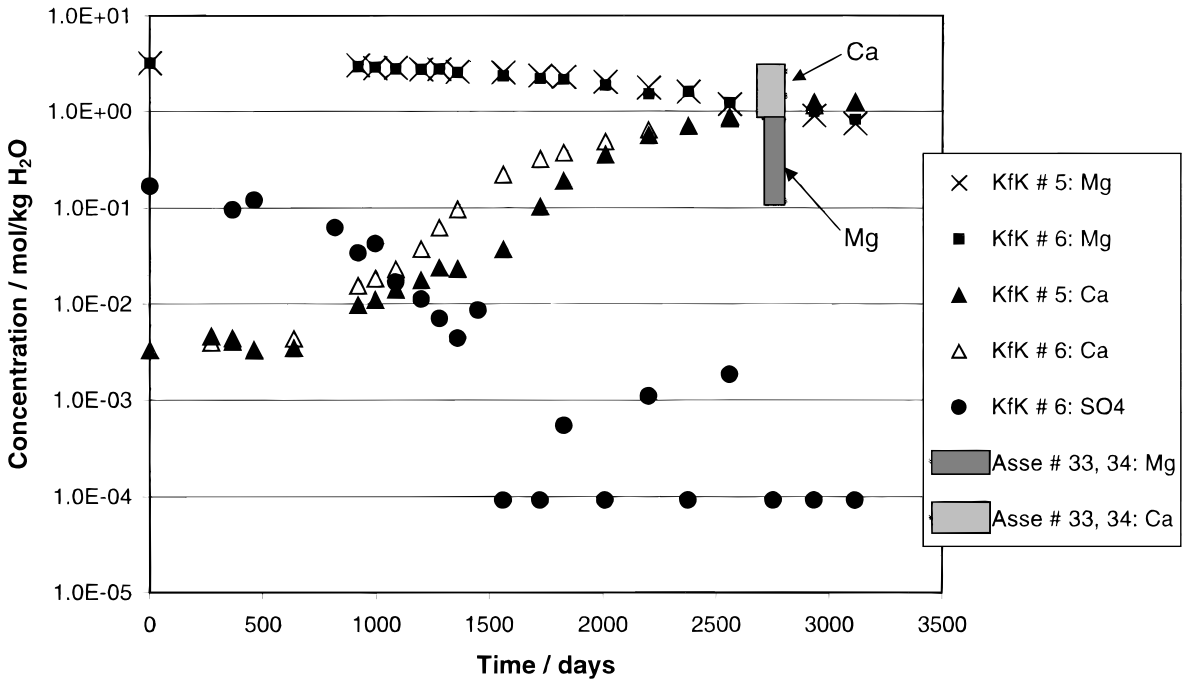

Fig. 1. Time dependence of the Ca, Mg, and SO_4 concentrations for KfK and Asse samples leached in Q-brine. Scattered symbols = KfK samples; boxes = Asse samples. Concentrations of Ca determined for samples KfK 5 and 6 were almost identical.

Downloaded by [the LANL Research Library] at 15:19 16 November 2017

III. PHENOMENAL FINDINGS

III.A. Interaction Between Waste Forms and Brines

In the KfK experiments, interactions between the waste forms and the brines were determined by periodically measuring the Ca, Mg, and SO_4 concentrations of the corroding brines for samples KfK 5 and KfK 6. The time dependence of the concentrations of both KfK experiments are shown in Fig. 1. After 1000 days, [Ca] was found to be ~0.02 mol/kg H_2O and 1.25 mol/kg H_2O after 3000 days. Parallel to this process, [SO_4] decreased by more than two orders of magnitude from 0.17 mol/kg H_2O at 1000 days to 10^{-4} mol/kg H_2O after 3000 days. The evolution of concentrations of main components is not available for the Asse experiments. In the Asse tests, the brine compositions were analyzed only once—on the 2767th day—for Asse sample Nos. 33 and 34. Measurements of these two samples at different levels from the bottom showed a significant scatter of data between 0.118 and 1.46 mol/kg H_2O for Mg and between 1.45 and 2.60 mol/kg H_2O for Ca. This scatter was a result of the mixing-sampling procedure. Mixing of the solutions resulted in higher concentrations of both elements. After filtration of the liquid samples, reduced concentrations were found.

In Fig. 1, the Mg concentration decreases continuously over time for KfK sample Nos. 5 and 6. The pH of the KfK experiments rose slightly from 6.5 to 7.2. the pH and the redox potential (Eh) of the Asse experiments were determined in 1998. Until then, the duration of the experiment was up to 19 yr. The results are shown in Fig. 2. The Asse tests showed no significant variations between those samples immersed since 1979 and those from 1989. The only differences were correlated with the initial brine compositions. Measured pH in Q-brine samples[d] ranged between 6.3 and 8.3; the corresponding Eh values were between +290 and +120 mV. Scatter of pH and Eh in NaCl-brines was lower. The pH was found to be between 11.9 and 11.3 and Eh from −47 to −58 mV. The samples immersed in tap water also showed a low scatter, i.e., $12.6 \leq pH \leq 12.9$ and $-19.7 \leq Eh \leq -58$ mV. The slope of the trend line Eh versus pH for all samples was computed to be −45.4 mV, which is larger than the theoretical value of −59.2 mV. However, a simple Nernst equation cannot be assumed because the apparent "equilibrium" potential is not necessarily the result of one single process.

A few samples of the Asse tests were analyzed for two other important components of cement: Al and Fe.

[d] In this context, the expressions Q-brine samples or NaCl-brine samples mean samples that were exposed initially to these brines. Of course, during the dissolution processes of the cemented waste forms, the initial brine composition changed significantly.

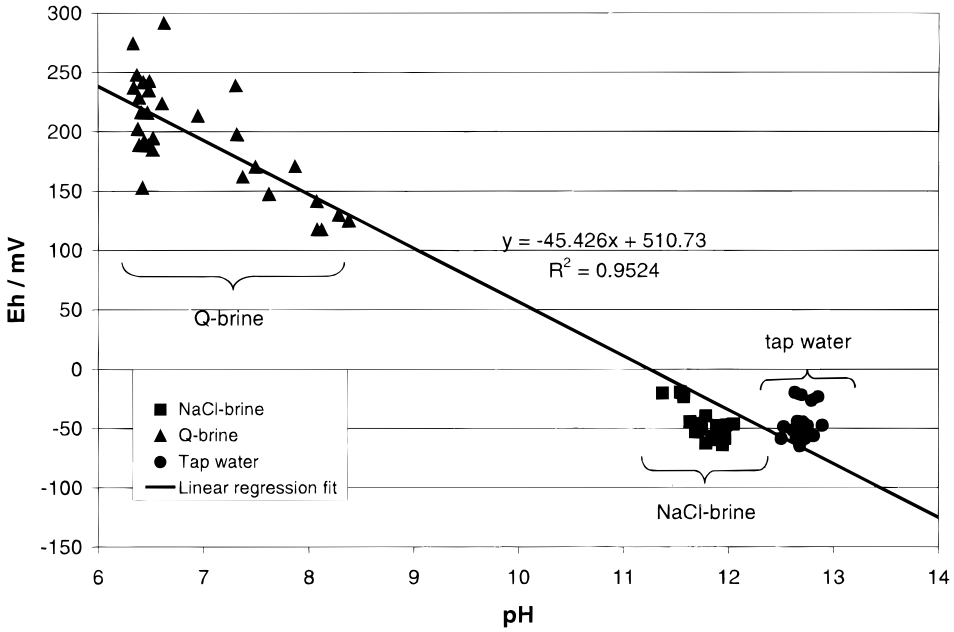

Fig. 2. Measured Eh-pH dependencies of the Asse samples corroded in the Q-brine, NaCl-brine, and in tap water after storing for periods between 9 and 19 yr.

Total iron content in Q-brine samples having a pH between 7 and 8.6 was found to be $\sim 1 \times 10^{-2}$ mol/kg H_2O. In NaCl-brine, iron concentrations were about three orders of magnitude lower (Fig. 3). Figure 2 shows that Eh is correlated to pH and not significantly to a specific redox reaction. Therefore, the differences in the iron concentrations are determined by the pH in the brines. [Si] was not analyzed.

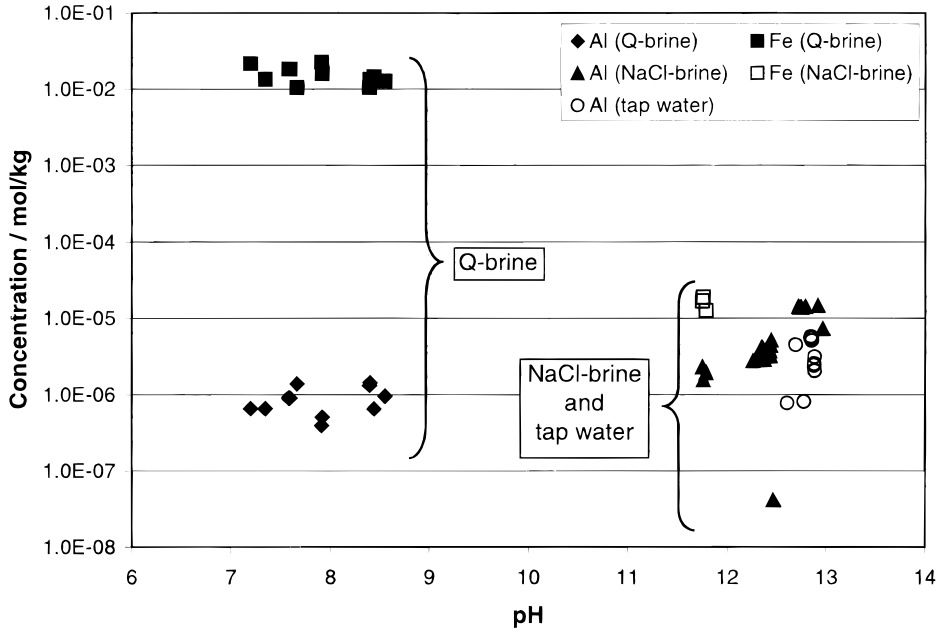

Fig. 3. Measured concentrations of Al and Fe in the Asse samples.

Downloaded by [the LANL Research Library] at 15:19 16 November 2017

Downloaded by [the LANL Research Library] at 15:19 16 November 2017

III.B. Self-Shielded Concrete Waste Container

Two self-shielded concrete waste containers were immersed into Q-brine (Table II) at 40°C. Both samples were inspected regularly. After 5.5 yr, the concrete containers showed the formation of a 4 to 5 mm thick layer at their top surfaces. Below this, a 2-mm layer of corroded concrete was detected. The cylindrical walls showed negligible corrosive attack. After 7.3 yr, some material had crumbled from the corners. The solution was clear, except for some precipitated $Mg(OH)_2$ flocs. In general, the concrete containers were in an adequate condition; the only weak point was the poured cement material used for filling the gaps. After 10.9 yr, the experiments were terminated, and samples were removed from the solution and cut along the cylindrical axis.

As can be seen by comparing the concentrations in Tables II and III, the $[Mg^{2+}]$ decreased by a factor of almost 2 and $[SO_4^{2-}]$ by a factor of 4.5 during the leaching period. These concentrations are different from those determined for cemented waste forms. These results indicate a reduced corrosion rate due to the low porous concrete used as shielding material. Cs^+ and NO_3^-, which were components of the simulated waste form, could not be detected in the solution after 10.9 yr. The progress of corrosion was determined visually and by means of measurements of the pressure resistance (ricochet hardness with a Schmidt hammer). Significant differences were found in those parts of the concrete canister filled with poured cement material.

In these experiments, the changes of the composition of the corroding Q-brine was less significant than that found in leaching experiments of cemented waste forms. The porosity of the concrete of the cylindrical wall was very low. Hence, exchange processes and correlated corrosion did not play a significant role within the period of the experiments. On the other hand, parts of the lid that had been filled with a rather porous cementitious material as sealing compound showed strong corrosive attack, which would lead to a loss of tightness. From the measured data, the tightness of a self-shielded concrete waste container can be expected only for a period of 30 to 50 yr. The durability of the concrete of the cylindrical walls used as radiation shielding is considerably longer.

III.C. Investigation of Solid Phases

Crystalline solids were sampled from the upper surface of the sample No. 27, which had been exposed to the leaching process in NaCl-brine for more than 6 yr at this time. Part of the specimen was dried carefully and ground for X-ray diffractometry; another part was prepared as thin sections for microscopic investigations. The following minerals could be identified by X-ray diffraction analyses: portlandite and halite (NaCl). Portlandite was precipitated during the corrosion process. Halite, which was present in the leachant, precipitated as a consequence of the drying of the specimens. Other solid phases could not be identified.

Thin sections for microscopic investigation were prepared from pure OPC samples (No. 9) stored in Q-brine and from sample No. 10, which was leached in NaCl-brine. All thin sections showed numerous cracks and changes of color at the crack surfaces. The cracks were partially filled with precipitated salt minerals. Precipitated salt was found in the pores of the cement matrix itself. By means of polarization microscopy, changes of the hardened cement could be shown. However, it was not possible to determine variations in the chemical composition of the material or to determine the mineralogical composition.

Up to now, these full-scale simulated waste form blocks are not disturbed. Drill cores and cuts of the samples will be available after termination of the leaching experiments. At this time, detailed investigations of the solids including element profiles and profiles of the mineralogical compositions will be performed.

III.D. Cs Release

The experiments at Asse and KfK were initially designed to determine the Cs release. For this purpose, trace amounts of inactive Cs and radioactive ^{137}Cs were added to several samples. The samples considered here (KfK 5 and 6; Asse sample Nos. 28 and 29) had approximately the same W/C ratio of 0.43.

Both experiments in Q-brine showed that after 10 to 19 yr of immersion time, the Cs is distributed between the waste forms and the attacking brines. To compare different types of experiments using inactive Cs or

TABLE III

Chemical Composition (mol/kg H_2O) of the Corroding Solutions of Two Self-Shielded Concrete Containers (VBA) After 10.9 yr*

mol/kg H_2O	Mg^{2+}	Ca^{2+}	K^+	Na^+	Cl^-	SO_4^{2-}	pH
VBA 1	2.42	3.3×10^{-3}	0.50	0.25	6.24	6.7×10^{-2}	6.9
VBA 2	2.47	2.9×10^{-3}	0.42	0.25	6.21	6.9×10^{-2}	6.9

*Initial brine composition corresponds to Q-brine in Table II.

low quantities of radioactive ^{137}Cs, the release of Cs in Fig. 4 is given in relative units (percent). Equation (1) was applied for computation of relative Cs release $\tilde{A}$ for active samples:

$$\tilde{A} = \frac{A \cdot m}{A_0 \cdot e^{-\lambda \cdot t}} \cdot 100\% \ , \qquad (1)$$

where

A = measured activity of the brine

A_0 = initial Cs activity of the sample

m = mass of the leachant

λ = decay constant of Cs

t = time since preparation of the samples.

The KfK samples showed a release of ~60% of Cs at a concentration of 0.04 mol/kg H_2O. The Cs release after 4527 days was measured to be 28.2 and 38.0% for the Asse sample Nos. 28 and 29, respectively. Most recent measurements, after 5034 days, showed a Cs release of ~58% for sample No. 28. Mechanical disintegration or cracks were not yet detected. From an inactively doped sample with a lower W/C ratio of 0.32, ~10% of Cs was released into the Q-brine after 3600 days. After this, Cs release remained almost constant up to 6441 days, at ~11%.

One can assume that the higher storage temperature of the KfK samples influenced the observed Cs release behavior. After ~600 days, the KfK samples showed an increase of the Cs release curve indicating changes in the release mechanism. It could be found by visual inspection that after this test period, the surface area of the samples had increased by the formation of cracks.

III.E. Uranium Release

Uranium release was investigated for several samples (Nos. 25, 26, and 27 and 31 through 34) at Asse. The total inventory was ~1 kg of natural uranium, as $(NH_4)_2U_2O_7$, in the test blocks. The results for the Q-brine tests at Asse are given in Fig. 5. Significant differences were found for the samples prepared and stored in 1984 (Nos. 25 and 26) and those prepared in 1989 (Nos. 33 and 34). Measured U concentrations differ by more than a factor of 400 after a storage period of 2700 days. The reason for the difference is not clear. The W/C ratios of the sample Nos. 25 and 26 were 0.30 and 0.34, and 0.50 for both sample Nos. 33 and 34. If kinetically controlled processes play a role, a reverse behavior would be expected. Measured uranium concentrations did not depend on the sampling positions of the leachant containers.

The results for leaching in NaCl-brine are shown in Fig. 6. Although the absolute U concentrations measured in NaCl-brine were significantly lower as in Q-brine, a similar behavior of uranium release was observed for the

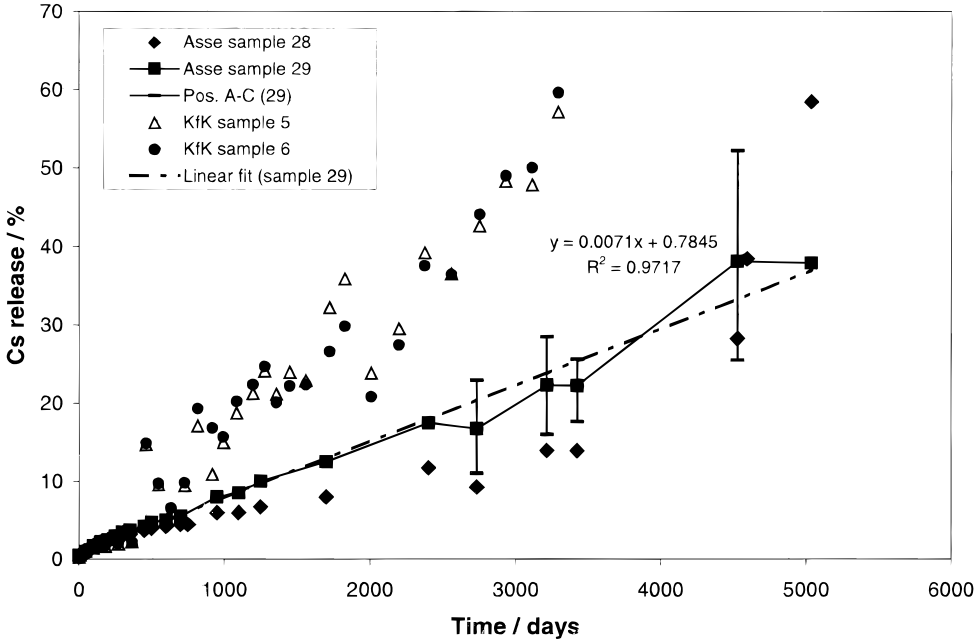

Fig. 4. Determination of the Cs release rate from full-scale cemented waste forms in Q-brine. Sample No. 29 indicates mean values; the vertical bars (positions A–C) represent the variations of concentrations measured at the top, middle, and bottom positions in the leachant container. Asse samples: T = 28°C; KfK samples: T = 40°C.

Downloaded by [the LANL Research Library] at 15:19 16 November 2017

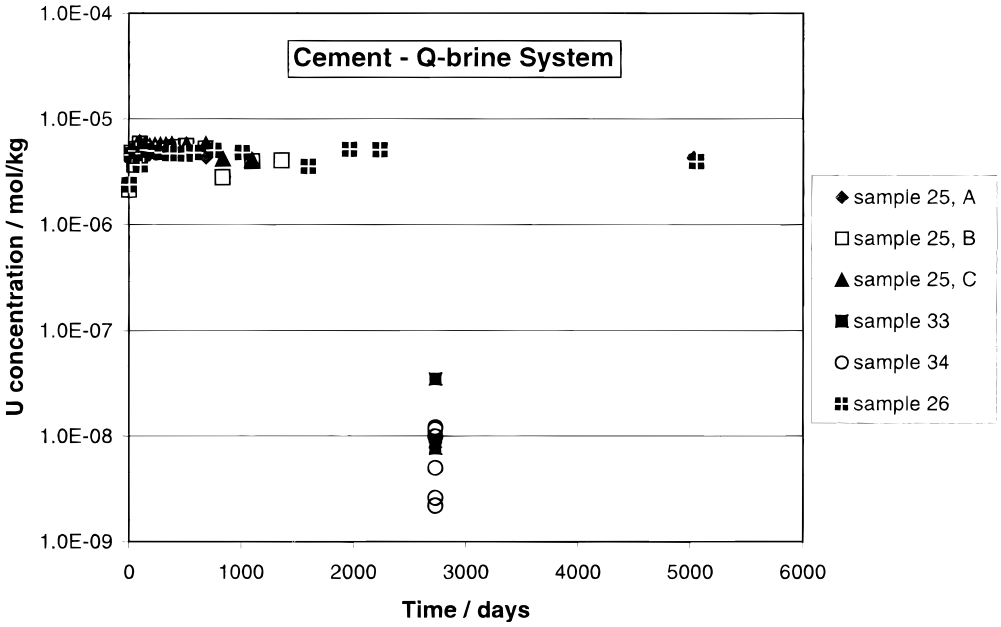

Fig. 5. Uranium release from cemented waste forms in Q-brine obtained by the Asse tests. For sample 25, A = top position in the leachant container; B = middle position; and C = bottom position.

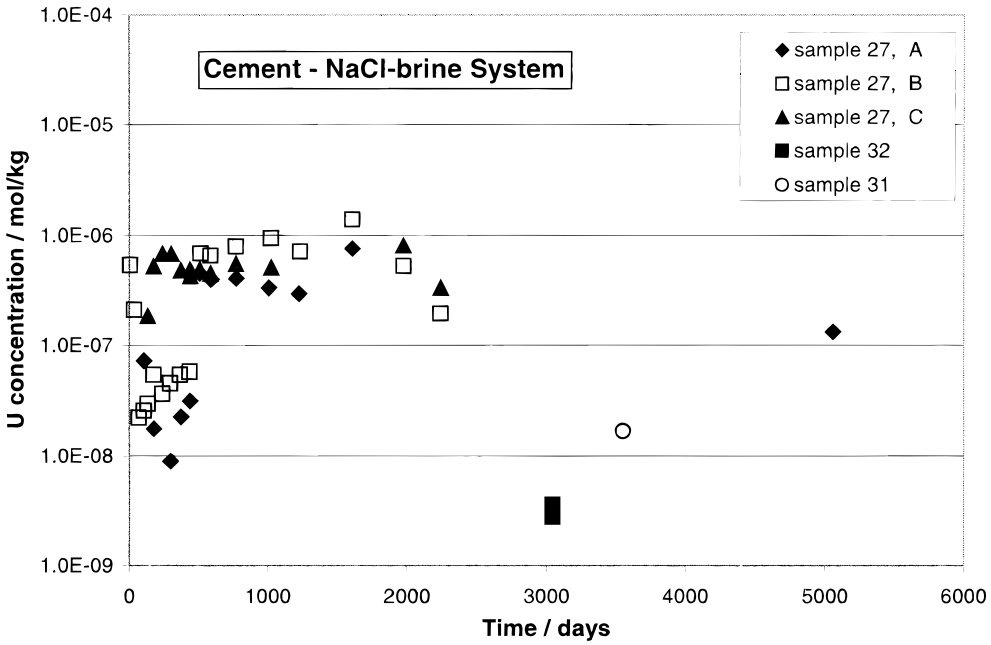

Fig. 6. Uranium release from cemented waste forms in NaCl-brine measured in the Asse tests. For sample 27, A = top position in the leachant container; B = middle position; and C = bottom position.

two series of experiments. In NaCl-brine, the samples prepared in 1989 showed a much lower U release than the others. The reason for the different behavior of the two series of tests is not yet clear. Analyses of the solid matrix are not yet available. In the NaCl-brine tests, measured uranium concentrations showed a slight variation of the U concentration depending on vertical sampling positions in the leachant container. However, it was not possible to obtain a correlation between the U concentration and the vertical level.

Downloaded by [the LANL Research Library] at 15:19 16 November 2017

Downloaded by [the LANL Research Library] at 15:19 16 November 2017

III.F. Neptunium Release

Full-scale samples containing Np (3.7×10^6 Bq per sample) have been prepared and stored in Q-brine and NaCl-solution. Time dependencies of measured Np concentrations in the solutions are not available. The latest measurements in 1998, after 9 yr leaching in the NaCl system, yielded a Np concentration below the detection limit of 0.013 ng/ml (5×10^{-11} mol/kg H_2O). In the Q-brine system, however, a concentration of 0.047 ± 0.004 ng/ml was measured by ICP-MS (1.8×10^{-10} mol/kg H_2O). This value exceeds the detection limit by a factor of ~3.

IV. INTERPRETATION OF RESULTS AND DISCUSSION

The results presented in the preceding sections allow different interpretations: Cs release and the investigations of the self-shielding concrete containers give information about the durability of these wastes in the salt solutions under consideration. The U and Np data allow an interpretation of the radionuclide concentrations and possible solids by thermodynamic modeling.

IV.A. Modeling the Interactions Between Cement and Brines

Interpretation of the radionuclide concentrations and possible solid phases requires thermodynamic modeling. Geochemical model calculations using the EQ3/6 Rel.7.2a package[15] were performed assuming a thermodynamic equilibrium between the solutions and solid phases. The initial brine composition, including all species involved in further reactions, was computed first. Then, to simulate corrosion of cemented waste, a linear dissolution model was chosen, infinitesimal amounts of a "special reactant" having the composition given in Table IV were "added" to the brines, and the equilibrium was determined by EQ6 computations. These infinitesimal steps of the EQ6 run (zi) correspond to the progress of cement dissolution. All simulations were performed for the temperature of 25°C.

For modeling purposes, the tabulated overall compositions of OPC clinker were used.[16] From the data of the cement clinker, the composition of a cemented waste form with a W/C of 0.4 and a load of 10 wt% waste salts was calculated. Cemented waste containing 0.02 mol/kg of homogeneously distributed uranium was considered.

In the OPC clinker, CaO and SiO_2 are present in the form of tricalciumsilicate or dicalciumsilicate in concentrations of ~60 and 20 wt%, respectively. In the presence of water, during the hydration process, these minerals react to give 2 and 1 moles portlandite ($Ca(OH)_2$), respectively. For this reason, an equilibrium of NaCl-brine and a magnesium rich brine with portlandite, the most abundant phase of hydrated cement, or with the special reactant given in Table IV, was computed using an extended Pitzer database of EQ3/6 Rel.7.2a. The detailed results are reported elsewhere.[17]

TABLE IV

Composition of the Cemented Waste Forms

	Composition of OPC (wt%)	Composition of Waste Forms (mol/kg)
CaO	64	7.34
SiO_2	20	2.14
Al_2O_3	5	0.63
Fe_2O_3	2.5	0.20
MnO	0.1	0.01
MgO	1.5	0.24
SO_3	2.5	0.20
O		43.56
H		44.44
U		0.02

The initial Ca concentration of the Q-brine was fixed by an equilibrium with the natural mineral polyhalite ($K_2MgCa_2(SO_4)_4 \cdot 2H_2O$). This phase was detected in short-term corrosion tests. Initial pH of the Q-brine-cement system was computed to be ~7. Figure 7 reveals the results of the simulations of cement dissolution. The figure shows the concentrations of the dissolved elements and the pH depending on the dissolution progress, which is expressed by the infinitesimal steps of the EQ6 run (zi).

Following the reaction of 2.8×10^{-4} kg of cement, the calculated pH increased to 8.7 and remained constant until 0.7 kg of cement had reacted. The computed Mg concentration also remained constant until ~0.7 kg cement had been dissolved. Simulation of further reaction showed that the computed pH increased up to 11.8, while the Mg concentration dropped from the initial concentration in the Q-brine to 7×10^{-2} mol/kg. Computed Ca concentration showed an inverse behavior: An increase from an initial Ca concentration of 1.4×10^{-4} to >1 mol/kg at pH 8.6 was computed. After dissolution of 1 kg of cement, the dissolved Ca concentration was near 3 mol/kg. At this point, the sulfate content in the solution was computed to be $\sim 5 \times 10^{-4}$ mol/kg. The silicate concentration reached a maximum value of 0.1 mol/kg after corrosion of 0.05 kg cement and then dropped to 7×10^{-6} mol/kg. Solid phases controlling the ion concentrations in the simulation are anhydrite ($CaSO_4$) for sulphate, portlandite, and calcium-silicate-hydrate phases (CSH), with a Ca-to-Si ratio of 0.8:1 and 1.1:1 for Ca and Mg-oxychloride ($Mg_2Cl(OH)_3 \cdot 4H_2O$), as well as brucite ($Mg(OH)_2$) for Mg. As shown in Fig. 8, X-ray diffraction analysis for cement samples corroded in Q-brine can be compared to the simulations. The com-

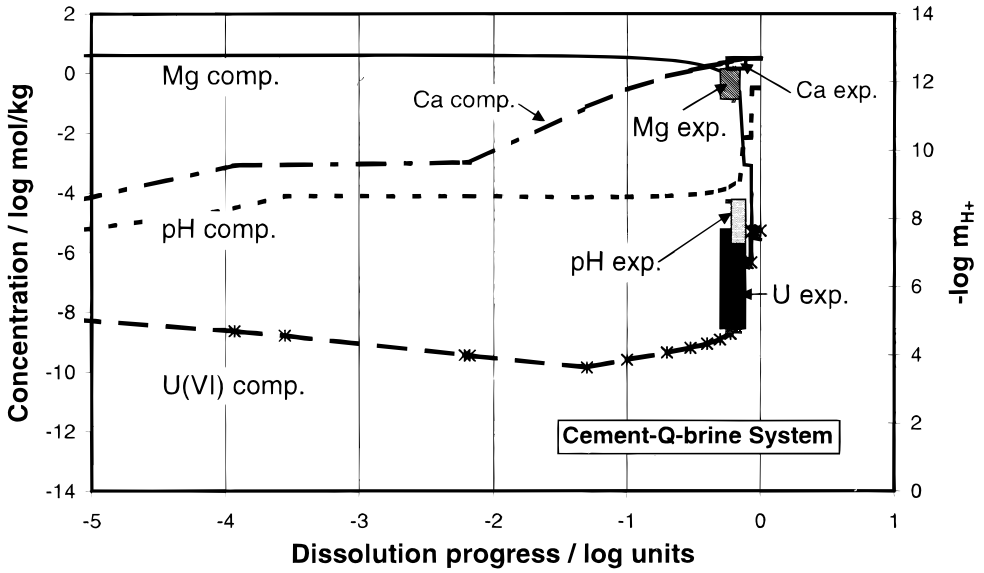

Fig. 7. Computed and measured element concentrations in the cement–Q-brine system.

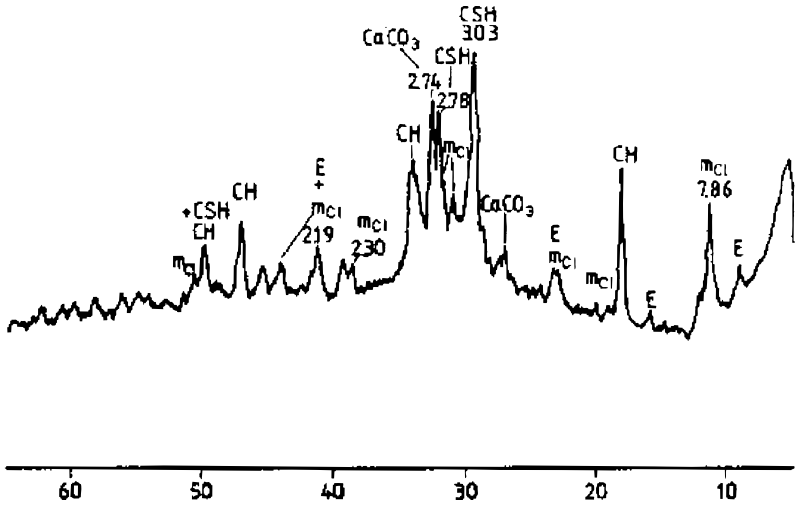

Fig. 8. The X-ray diffraction analysis of a cemented ILW sample corroded in Q-brine at 40°C for 90 days: CH = portlandite; m_{Cl} = Friedel's salt; and E = ettringite.

Downloaded by [the LANL Research Library] at 15:19 16 November 2017

puted solid phases presented in Fig. 9 are portlandite, brucite, and Mg-oxychloride and CSH phases. Friedel's salt ($3CaO \cdot Al_2O_3 \cdot CaCl_2 \cdot 12H_2O$) and hydrotalcite ($Mg_6Al_2Cl_2(OH)_{16}$) were computed but not shown in the figure. The experiments were performed under aerobic conditions. For this reason, the formation of carbonate phases such as calcite or vaterite ($CaCO_3$) could be expected. Friedel's salt and clinker phases (CSH), quartz (SiO_2), and a small quantity of ettringite ($Ca_6Al_2(SO_4)_3(OH)_{12} \cdot 26H_2O$) could also be identified.

In the NaCl-brine, the pH in the simulation reached an equilibrium value of 12.5 following the reaction of a small amount of cement. The initial Ca concentration (Table II) remained constant until ~1 g of cement was corroded. At higher degrees of corrosion, the Ca concentration increased, ending at 0.1 mol/kg. During the course of the simulated corrosion progress, Mg precipitated, and the solution concentration decreased to 10^{-6} mol/kg. Solids controlling the Ca concentration are portlandite and CSH(1:1). Up to the corrosion progress of log $zi = -2.7$ (corrosion of $10^{-2.7}$ kg/cemented waste form), Mg remained in solution. With increasing pH, the calculation predicted a precipitation of brucite, thereby reducing the total Mg concentration to below 10^{-6} mol/kg. The silicate

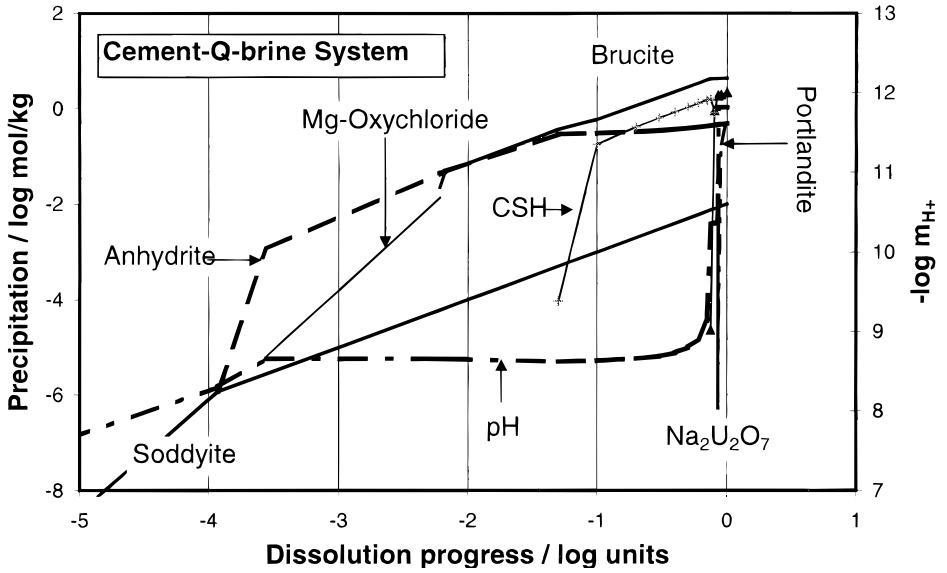

Fig. 9. Computed mineral precipitation in the cement–Q-brine system.

concentrations were computed between 0.1 and 4 mmol/kg. The computed evolution of the NaCl-brine due to the corrosion of cemented waste forms is shown in Fig. 10.

In the database used for these computations, aluminum was represented by the dissolved $Al(OH)_4^-$ species. Pitzer interaction coefficients for this ion are available for the main components of the brines.[18,19] The [Al] was computed to be 6×10^{-7} mol/kg H_2O in NaCl-brine and in Q-brine; the maximum Al concentration was $\sim 1 \times 10^{-8}$ mol/kg H_2O, decreasing after dissolution of 1 kg of cement to 5×10^{-10} mol/kg. Hydrotalcite and Friedel's salt were found to be the solids controlling Al concentrations. For NaCl-brine, measured Al concentration varies by a factor of 2 below to a factor of 20 above computed concentrations, and in Q-brine the computed value underestimates Al concentration by a factor of 100 (see Fig. 3).

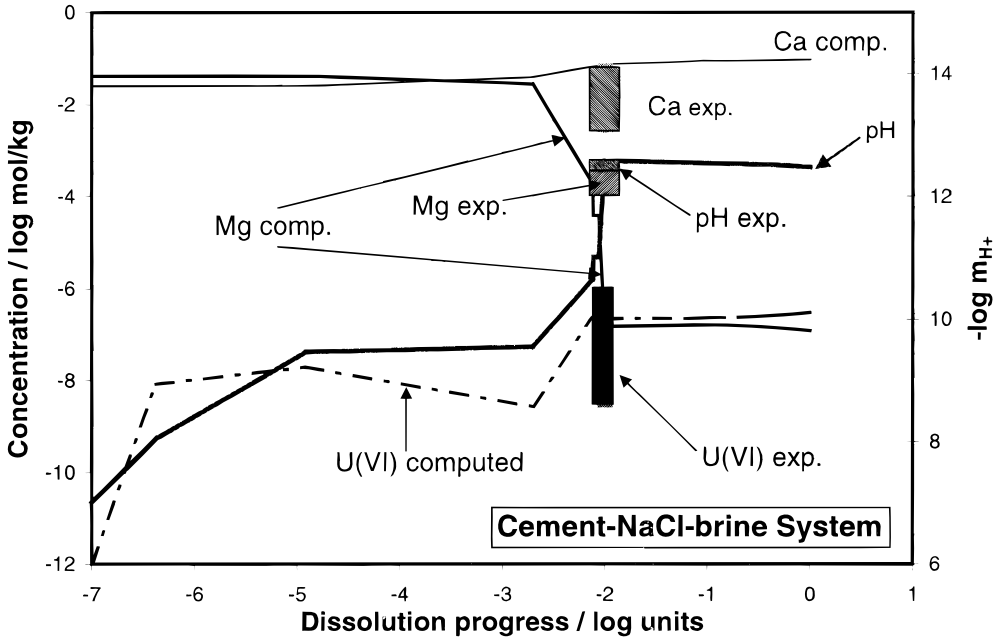

Fig. 10. Computed and measured element concentrations in the cement–NaCl-brine system.

Downloaded by [the LANL Research Library] at 15:19 16 November 2017

Modeling of Al concentration requires the identification of solids that control the solubility. In X-ray diffraction analysis of corroded cement, Friedel's salt was detected after corrosion periods of 90 days (Fig. 8). However, if this mineral phase remains stable over the experimental period of almost 20 yr under consideration of the changed leachants, it has not yet been determined. Different solid Al phases or mixed phases may be significant.

IV.B. Cesium Release

Assuming Cs to be a key nuclide indicating transport processes within the cemented waste forms, measured Cs release can be applied to evaluate the time dependency of the process. Figure 4 shows that Cs release is a linear process over long periods of time. Diffusively controlled processes may play a role for short terms only, e.g., less than 600 days for sample No. 29 and perhaps up to 10 yr for sample No. 28 in the experiments at Asse. Samples at KfK (Nos. 5 and 6) also show a linear Cs release (see Fig. 4).

The Cs release behavior indicates that cement has no retention capacity for cesium. Within the test periods, Cs is distributed between the solution and the corroded cement. However, the pore volume of the cement, which is related to its W/C ratio, influences the release rate. Higher pore volume gives rise to faster Cs release. The same process is observed for the Ca release from cement. Some samples prepared with a W/C of 0.24 showed a very limited increase of Ca in the solution. Visual inspection of these samples did not reveal any degradation after 19 yr.

IV.C. Uranium

The computations were aimed at determining the radionuclide concentrations in the corroding solutions. U(VI) was chosen as a representative radionuclide. Uranium interaction parameters, which are relevant for the highly concentrated brines, are available for certain U-species in the Pitzer database. Data on hydroxo- and silicate solid uranium phases are available as well. Reactions of the pure $CaO\text{-}SiO_2$ system with schoepite ($UO_3 \cdot 2H_2O$) at 85°C have been investigated experimentally.[20] These experiments showed that several U phases of the type $CaO\text{-}UO_3\text{-}SiO_2\text{-}H_2O$ control the U solubility in the high-pH region. The solubilities varied between 10^{-5} and 10^{-9} mol/kg, depending on the Ca/Si ratio of the solids.

Initally, Eh-pH diagrams for uranium were computed, taking into account the measured U concentrations (Fig. 5) and the ionic strength of the solutions (see Table II). Results for the Q-brine are shown in Fig. 11. This diagram was computed for the ionic strength of Q-brine. As expected, the effect of different ionic strengths of the brines was not significant, because only the chemical activity of water is considered in this type of diagram. For this reason, measured Eh-pH data for NaCl-brine and Q-brine uranium tests could be plotted in the same diagram. The Eh-pH diagram for uranium shows the stability and predominance of different dissolved uranium species over the possible ranges of pH and redox potential. The measured pH depends on the amount of dissolved portlandite in the experiments. Measured redox potentials of the brines depend on the availability of dissolved oxygen $O_2(aq)$. As shown in Sec. III.A, different processes may contribute to the $O_2(aq)$ concentration. The $O_2(aq)$ concentration may be influenced by the tightness of the lid systems of the leachant containers or by the presence of iron. Trace concentrations of dissolved uranium do not change the redox potentials. Measured Eh and pH of the Asse sample Nos. 25, 26, and 27 and 31 through 34 indicate the stability of U(VI) in both brines. Therefore, the differences in the uranium concentrations between the experiments reported in Figs. 5 and 6 cannot be explained by the redox state. Carbonate concentration by equilibrium with the CO_2 gas in the air results in calculated CO_3^{2-} concentrations of below 3×10^{-6} mol/kg for the brines under consideration. The EQ3/6 computations showed that carbonato-uranium complexes were not significant under the conditions of the cement-brine systems. The Geochemist's Workbench (GWB) code[21] and the data for dissolved U species given in Table V and for solids in Table VI were used for the Eh-pH diagram.

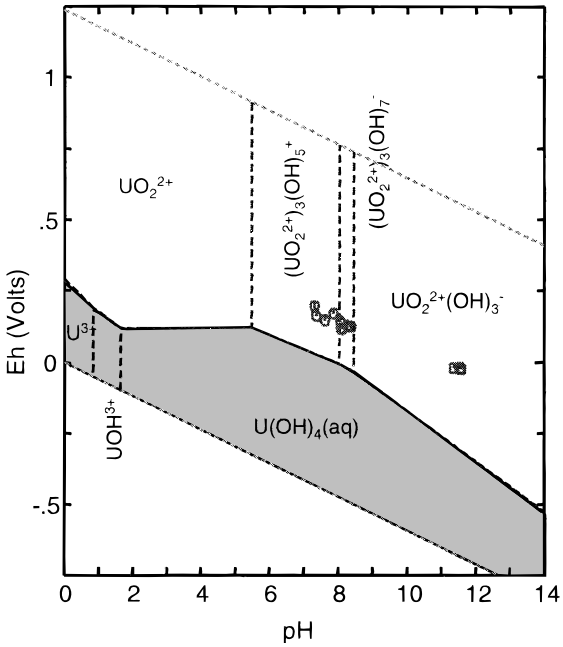

Fig. 11. The Eh-pH diagram for uranium at 25°C, $[U] = 10^{-6}$ mol/kg. Markers indicate measured Eh-pH data of full-scale uranium experiments stored in NaCl-brine and in Q-brine.

Downloaded by [the LANL Research Library] at 15:19 16 November 2017

TABLE V

Dissolved U Species Considered in EQ3/6 and GWB Computations

Reaction	log *K*	Reference
$U_3^+ \Leftrightarrow -H^+ + U^{4+} + 0.5H_2O - 0.25O_2(aq)$	30.357	22
$UO_2^+ \Leftrightarrow -3H^+ + U^{4+} + 1.5H_2O + 0.25O_2(aq)$	−15.07	22
$UO_2^{2+} \Leftrightarrow -2H^+ + U^{4+} + H_2O + 0.5O_2(aq)$	−33.784	22
$UO_2(OH)_3^- \Leftrightarrow -3H^+ + UO_2^{2+} + 3H_2O$	19.223	22
$UO_2(OH)_4^{2-} \Leftrightarrow -4H^+ + UO_2^{2+} + 4H_2O$	33.030	22
$(UO_2)_2(OH)_2^{2+} \Leftrightarrow -2H^+ + 2UO_2^{2+} + 2H_2O$	5.680	22
$(UO_2)_3(OH)_4^{2+} \Leftrightarrow -4H^+ + 3UO_2^{2+} + 4H_2O$	11.929	22
$(UO_2)_3(OH)_5^+ \Leftrightarrow -5H^+ + 3UO_2^{2+} + 5H_2O$	15.586	22
$UO_2(OH)_2(aq) \Leftrightarrow -2H^+ + UO_2^{2+} + 2H_2O$	11.500	23,24
$(UO_2)_3(OH)_7^- \Leftrightarrow -7H^+ + 3UO_2^{2+} + 7H_2O$	31.051	22
$U(OH)_4 \Leftrightarrow -4H^+ + U^{4+} + 4H_2O$	4.570	22
$UOH^{3+} \Leftrightarrow -H^+ + U^{4+} + H_2O$	0.547	22

TABLE VI

Solid U(VI) Phases Considered in the EQ3/6 Computations

	Solid		log *K*	Reference
Hydrate	Schoepite	$UO_3 \cdot 2H_2O$	5.37	25
	Schoepite-dehydrated	$UO_3 \cdot 0.9H_2O$	5.00	15
	Compreignacite	$K_{0.33}UO_{3.165} \cdot 1.8H_2O$	6.33	26
	Becquerelite	$Ca_{0.16}UO_{3.16} \cdot 1.8H_2O$	7.13	26
Nonhydrous		$Na_2U_2O_7$	26.0	25
		$CaUO_4$	15.93	15
Silicate	Soddyite	$(UO_2)_2(SiO_4) \cdot 2H_2O$	5.74	27
	Na-Weeksite	$Na_2(UO_2)(Si_2O_5)_3 \cdot 4H_2O$	1.50	27
	Na-Boltwoodite	$Na_{0.3}K_{0.7}(H_3O)(UO_2)(SiO_4) \cdot H_2O$	5.82	27
	Uranophane	$Ca(UO_2)_2(SiO_3OH)_2 \cdot 5H_2O$	9.42	27

As described earlier, uranium was considered to be distributed homogeneously in the cemented waste form, and it was considered to be one part of the special reactant cement (see Table IV). The results of the computations are shown in Figs. 7 and 11, together with the experimental findings. Computations were performed under the assumption that $Na_2U_2O_7$ is the solubility-controlling phase. The range of measured values is indicated by a vertical bar in these figures. Experimental U(VI) concentrations range between 3×10^{-9} and 1×10^{-6} mol/kg in the cement–NaCl-brine system and from 2×10^{-9} to 5×10^{-6} in the cement–Q-brine system. For reaction-path modeling with the EQ6 code, relative reaction rates were applied, depending on the equilibrium conditions only. To compare the computations with the observed data, the experimental timescale had to be related to the computed reaction progress. This relation was defined by the correspondence of experimental and computed $[Ca^{2+}]$. The quality of this relation could be tested by comparisons of computed and measured $[Mg^{2+}]$ and pH (Figs. 7 and 11). For the cement–Q-brine and NaCl-brine cases, the computed U(VI) concentrations, with $Na_2U_2O_7$ as the limiting solid phase, agreed well with the experimental findings.

After an initial increase to 10^{-8} mol/kg, the U(VI) concentration decreased by 2 orders of magnitude in the Q-brine samples at a corrosion progress of 0.05 kg ($\log zi = -1.3$). This effect is correlated to an increase of dissolved silicate and, consequently, in the precipitation of soddyite. As the reaction of cement proceeded, the U(VI) concentration increased to $\sim 10^{-5}$ mol/kg, controlled by $Na_2U_2O_7$. For Q-brine with ~ 0.71 mol/kg K^+, formation of compreignacite was not computed. If becquerelite would be considered as the solubility-limiting phase, the computed U(VI) concentration would be higher by about three orders of magnitude.

Downloaded by [the LANL Research Library] at 15:19 16 November 2017

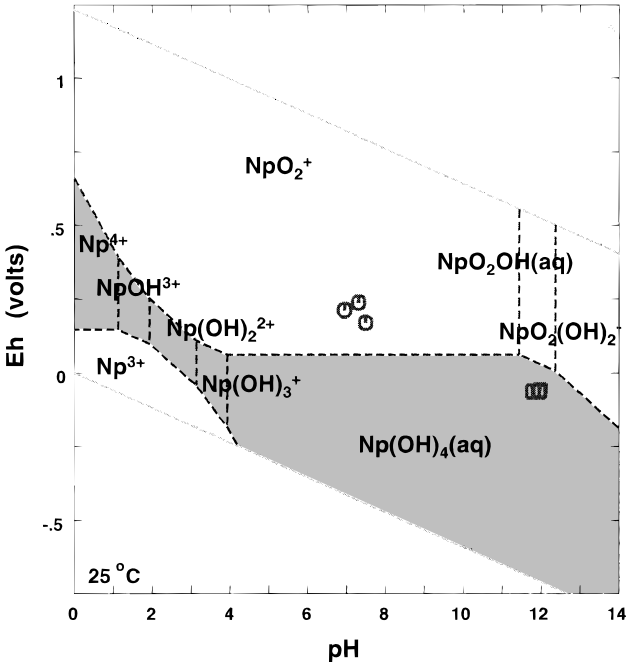

Fig. 12. Eh-pH diagram for neptunium at 25°C, $[Np] = 10^{-6}$ mol/kg. Markers indicate measured Eh-pH data of full-scale neptunium experiments stored in NaCl-brine and in Q-brine.

The solubility constant ($\log K$) of the yellow cake ($(NH_4)_2U_2O_7$) used in some experiments or the constant of the rather similar $K_2U_2O_7$ is not available in the main important database.[22] However, solubility data of $(NH_4)_2U_2O_7$ are reported in Ref. 28. If these solubility data are used to compute a "conditional" solubility constant, the resulting value is significantly higher than the one for $Na_2U_2O_7$. For this reason, one can conclude that sodium diuranate also controls uranium solubility in the case of yellow cake.

IV.D. Neptunium

For Np, a few measured concentrations close to the detection limit are available. Similar to uranium, the Eh-pH diagram for neptunium was computed at the ionic strength of the solutions under investigation (see Table II). The results are shown in Fig. 12. This diagram is based on thermodynamic data given in Tables VII and VIII and shows the stability and predominance of different dissolved neptunium species over the possible ranges of pH and redox potential. The measured Eh-pH values of the Np samples indicate the predominance of dissolved Np(V) for the Q-brine system, whereas for the NaCl-cement system, dissolved Np species may be in the tetravalent oxidation state. Therefore, detected Np concentration in the Q-brine experiment may be attributed to the pentavalent redox state.

Neptunium concentrations yielded by EQ3/6 computations depend on the reaction progress of the cemented waste form. As in the uranium case, comparisons of computations with observed data require a relation between the experimental timescale and the computed reaction progress. This relation was also defined by correspondence of experimental and computed $[Ca^{2+}]$. In contrast to the uranium results, this relation produced Np concentrations of 5×10^{-7} mol/kg H_2O, which exceeds the measured values (ICP-MS 1.8×10^{-10} mol/kg H_2O) by about a factor of 3000. In this case, the solid Np_2O_5 was assumed to control the Np concentration. Using NpO_2 as a solubility-limiting solid, the computed Np concentration is about one order of magnitude lower than in the case of Np_2O_5. The aqueous NpO_2OH complex was found to be most significant. Consideration of carbonate by an equilibrium with CO_2 gas in air did not result in significant concentrations of neptunium-carbonato species.

TABLE VII

Dissolved Np Phases Considered in the in EQ3/6 and GWB Computations

Reaction		log *K*	Reference
Np^{3+}	$\Leftrightarrow -1H^+ - 0.25O_2(aq) + 0.5H_2O + Np^{4+}$	18.289	29
NpO_2^+	$\Leftrightarrow -3H^+ + 0.25O_2(aq) + Np^{4+} + 1.5H_2O$	−9.868	29
NpO_2^{2+}	$\Leftrightarrow -2H^+ + 0.5O_2(aq) + H_2O + Np^{4+}$	−9.762	29
$NpO_2OH(aq)$	$\Leftrightarrow -1\ H^+ + H_2O + NpO_2^+$	11.305	30
$NpO_2(OH)_2^-$	$\Leftrightarrow -2H^+ + 2H_2O + NpO_2^+$	23.536	30
$Np(OH)_2^{2+}$	$\Leftrightarrow -2H^+ + Np^{4+} + 2H_2O$	2.8	29
$Np(OH)_3^+$	$\Leftrightarrow -3H^+ + Np^{4+} + 3H_2O$	5.8	29
$Np(OH)_4(aq)$	$\Leftrightarrow -4H^+ + Np^{4+} + 4H_2O$	9.6	29
$Np(OH)_5^-$	$\Leftrightarrow -5H^+ + Np^{4+} + 5H_2O$	14.3	29
NpO_2OH^+	$\Leftrightarrow -1H^+ + H_2O + NpO_2^{2+}$	5.2	29
$NpOH^{2+}$	$\Leftrightarrow -1H^+ + H_2O + Np^{3+}$	70	29
$NpOH^{3+}$	$\Leftrightarrow -1H^+ + H_2O + Np^{4+}$	10	29

Downloaded by [the LANL Research Library] at 15:19 16 November 2017

TABLE VIII

Solid Np Phases Considered in the in EQ3/6 and GWB Computations

Solid		log *K*	Reference
$Np(OH)_4$	$\Leftrightarrow -4H^+ + Np^{4+} + 4H_2O$	0.8103	29
Np_2O_5	$\Leftrightarrow -2H^+ + H_2O + 2NpO_2^+$	7.9902	29
NpO_2	$\Leftrightarrow -4H^+ + Np^{4+} + 2H_2O$	−7.8026	29
$NpO_2(OH)_2$	$\Leftrightarrow -2H^+ + NpO_2^{2+} + 2H_2O$	5.9851	29
$NpO_2OH(s)$	$\Leftrightarrow -1H^+ + H_2O + NpO_2^+$	4.5151	30
$NpO_2OH(am)$	$\Leftrightarrow -1H^+ + H_2O + NpO_2^+$	5.2151	30

V. CONCLUSIONS

The observations presented here for full-scale leaching experiments correspond well with the findings of laboratory-scale experiments, e.g., Refs. 10 and 12. As was stated, the leached activity measured in solutions of laboratory-scale and full-scale samples is quite reproducible, and the ratio of the sample surfaces to volumes of the leachant can be used as a scale factor. The full-scale leaching experiments confirmed that cemented waste forms do not have a retention capacity for cesium.

In this paper, additional conclusions can be drawn from the results of full-scale tests and the corresponding modeling studies that cover important aspects, such as the durability of cemented waste forms, radionuclide release, and the maximum radionuclide concentrations used in the context of performance assessment analyses:

1. Mechanical durability of the waste forms:
   a. Mechanical durability of the waste forms, in the sense that no significant formation of cracks or disintegration was observed, is estimated to be 10 to 20 yr for cemented waste forms in contact with Q-brine. Durability may be longer if the cemented waste is exposed to NaCl-brine, especially in the case of a low pore volume (low W/C).
   b. For self-shielded waste canisters, the lid system consisting of a high W/C cementitious product is identified to be the weak point. Radionuclide release from such canisters may occur after 30 to 50 yr. However, durability of the high-quality concrete of the cylindrical walls is considerably longer.
2. Radionuclide release:
   a. Cemented waste forms do not retain cesium. Cesium release follows a linear time function. Only for short periods, diffusion-controlled transport processes may be relevant.
   b. Concentration of uranium in the attacking solutions is controlled by solid phases. In the cement–Q-brine and NaCl-brine, uranium is stable in the hexavalent oxidation state. Computed U(VI) concentrations, with $Na_2U_2O_7$ as the solubility-limiting solid phase, agreed well with the experimental findings. Maximal U(VI) concentration is expected to be in the range of 10^{-5} mol/kg H_2O in Q-brine and $\sim 10^{-6}$ mol/kg H_2O in NaCl-brine. The database concerning the Pitzer parameters for uranium and neptunium and the corresponding solids should be further developed.
   c. Neptunium was measured to be present in concentrations close to detection limits. Computations resulted in significantly higher concentrations. The reason for this discrepancy has not yet been identified.
3. Geochemical milieu of the leachants:
   a. Computations showed that 1 ℓ of Q-brine has the ability to corrode 0.55 kg, and 1 ℓ of NaCl-brine can corrode ~0.009 kg of cemented waste forms. Comparison with experiments shows that Q-brine samples are corroded by >20 wt%, while NaCl-brine samples are corroded to a much lower extent of 0.3%.
   b. Comparisons between computed and measured cement corrosion-dissolution processes are possible, if the experimental timescale is related to the computed reaction progress. This relation was defined by the correspondence of experimental and computed $[Ca^{2+}]$ and tested by comparisons of computed and measured $[Mg^{2+}]$ and pH data. However, there is a strong need to examine and improve the database concerning the Pitzer parameters for dissolved Al and Si species and the corresponding solids.
   c. Because of the high concentrations of Mg^{2+} or Ca^{2+}, the CO_3^{2-} concentrations in these

Downloaded by [the LANL Research Library] at 15:19 16 November 2017

solutions is limited to below 3×10^{-6} mol/kg. The computations showed that the formation of uranium or neptunium-carbonato species will not play a significant role under the conditions considered.

The experiments described yielded a cement corrosion of more than 20 wt% within 14 yr of storage in Q-brine (Asse sample Nos. 28 and 29). A prediction of corrosion based on diffusively controlled transport processes was published in 1985 (Ref. 31). Data given in this paper estimated the extent of corrosion to be ~7 vol% (14 wt%) within 50 yr for a slag cement waste form. In the case of increased diffusion coefficients, which are relevant for OPC waste forms, the corrosion was estimated to be 7.5 vol% (15 wt%) within 10 000 days. The predictions remained below the observations mainly due to the fact that linear transport processes have to be taken into account.

The long-term, full-scale leaching experiments using cemented waste forms in different salt brines present a valuable pool of information that can be used in safety analyses. The phenomenological observations give information on the degradation and mechanical disintegration of waste forms. The experiments cover the relevant physicochemical phenomena including kinetic and thermodynamic aspects to test models applied in safety analyses for extrapolation of short-term observations to time periods relevant for the isolation of long-lived radioactive waste. In this context, continuation of long-term experiments is highly advisable.

ACKNOWLEDGMENT

Part of this work was supported by the Bundesamt für Strahlenschutz within the project: "Erstellung eines integrierten Nahfeldmodells von Gebinden hochaktiver Abfälle im Salzstock Gorleben: geochemisch fundierter Quellterm für HAW-Glas, abgebrannte Brennelemente und Zement."

REFERENCES

1. "Endlager Morsleben," Pressemitteilung 10/98, Bundesamt für Strahlenschutz (May 18, 1998).

2. R. STORCK, D. BUHMANN, R.-P. HIRSEKORN, T. KÜHLE, and L. LÜHRMANN, GRS-122, Gesellschaft fuer Reaktorsicherheit (1996).

3. "Kristallin-I, Conclusions from the Regional Investigation Programme for Siting a HLW Repository in the Crystalline Basement of Northern Switzerland," NAGRA 93-09E, Nationale Genossenschaft für die Lagerung Radioaktiver (1994).

4. G. G. LOOMIS, A. P. ZDINAK, and M. T. BUTTE, "Field-Scale Permeation Testing of Jet-Grouted Buried Waste Sites," presented at Waste Management '97, Tucson, Arizona, March 2–7, 1997.

5. "Lysimeter Study of Commercial Reactor Waste Forms: Waste Form Acquisition Characterization and Full-Scale Leaching," BNL-51613, Brookhaven National Laboratory (Feb. 1983).

6. J. MARCAILLOU, J. C. FAURE, A. BERNARD, and J. C. NOMINE, "Practice Followed at the Cadarache Nuclear Research Centre in the Conditioning of Solid Radioactive Wastes for Purposes of Temporary Storage While Awaiting Disposal," *Proc. Int. Symp. Conditioning of Radioactive Wastes for Storage and Disposal*, Utrecht, The Netherlands, June 21–25, 1982, IAEA-SM–261/6, International Atomic Energy Agency (1982).

7. D. C. PHILLIPS, R. KÖSTER, and G. DE-ANGELIS, "Radiation, Thermal and Mechanical Effects on Low and Medium Active Conditioned Waste," *European Conf. Radioactive Waste Management and Disposal*, Luxembourg, Luxembourg, April 22–26, 1985; see also *Radioactive Waste Management and Disposal*, p. 275, R. SIMON, Ed., Cambridge University Press, New York (1985).

8. A. BERNARD, A. BONNET, G. CORNEC, L. FARGES, and J. C. NOMINE, "Long-Term Leaching Tests on Full-Scale Blocks of Radioactive Wastes," *Nucl. Chem. Waste Manage.*, **3**, *3*, 161 (1982).

9. M. KIKUCHI, M. MATSUDA, T. NISHI, S. TAMATA, and T. IZUMIDA, "A High-Performance Cement for Solidification of Spent Ion-Exchange Resin," *Proc. Int. Conf. Nuclear Waste Management and Environmental Remediation: Vol. 3—Environmental Remediation and Environmental Management Issues*, Prague, Czech Republic, September 5–11, 1993, p. 177, R. BASCHWITZ, R. KOHOUT, J. MAREK, P. I. RICHTER, and S. C. SLATE, Eds., American Society of Mechanical Engineers (1993).

10. J. C. NOMINE, A. BILLON, and G. COURTOIS, "Leaching Scale Effect for Cement-Waste Forms," *Proc. 12th Int. Symp. Scientific Basis for Nuclear Waste Management*, Berlin, Germany, October 10–13, 1988, p. 431, W. LUTZE and R. C. EWING, Eds., Materials Research Society (1989).

11. H. HINSCH and F. KESSLER, "Leaching Experiments with Real-Scale Specimens in the Asse Abandoned Shaft. Period Covered: 1979–1985," GSF–1/85, Gesellschaft fuer Strahlen- und Umweltforschung (1985).

12. P. VEJMELKA, G. RUDOLPH, W. KLUGER, and R. KÖSTER, "Die Konditionierung radioaktiver Abfallösungen durch Zementierung," KfK 4800, Kernforschungszentrum Karlsruhe (1990).

13. B. KIENZLER and P. VEJMELKA, "Geochemische Modellierung der Korrosion von zementierten Abfallprodukten in Salzlösungen. Experimentelle Basis, Methoden und Ergebnisse," FZKA 6046, Forschungszentrum Karlsruhe (1998).

14. R. KÖSTER, "Cementation of Radioactive Wastes in the Federal Republic of Germany," *Proc. Waste Management '85, Vol. 2. Waste Policies and Programs, Low-Level Waste*, Tucson, Arizona, March 24–28, 1985, p. 487, R. G. POST, Ed., American Nuclear Society (1985).

Downloaded by [the LANL Research Library] at 15:19 16 November 2017

15. "EQ3/6, A Software Package for Geochemical Modeling, Version 7.2a" [software produced under the designated unclassified subject area (DUSA) "Yucca", 1990–1993], Lawrence Livermore National Laboratory (1992).

16. Verein Deutscher Zementwerke, *Zement Taschenbuch*, 48, Ausgabe, Bauverlag GmbH, Berlin, Germany (1984).

17. B. KIENZLER, "Modelling the Geochemical Milieu in a Rock Salt Repository in the Presence of Cement," *Proc. Radioactive Waste Products, RADWAP'97*, Würzburg, Germany, June 23–26, 1997, p. 197, R. ODOJ, J. BAIER, P. BRENNECKE, and K. KÜHN, Eds., Forschungszentrum Jülich (1998).

18. E. J. REARDON, "An Ion Interaction Model for the Determination of Chemical Equilibria in Cement/Water Systems," *Cement and Concrete Res.*, **20**, 157 (1990).

19. E. REVERTEGAT, F. ADENOT, C. RICHET, L. WU, F. P. GLASSER, D. DAMINOT, and S. A. STRONACH, "Theoretical and Experimental Study of Degradation Mechanisms of Cement in the Repository Environment," EUR 17642, Commission of the European Communities (1997).

20. L. P. MORONI and F. P. GLASSER, "Reactions Between Cement Components and U(VI) Oxide," *Waste Manage.*, **15**, 234 (1995).

21. C. M. BETHKE, *The Geochemist's Workbench, Version 3*, University of Illinois, Champaign-Urbana, Illinois (1998).

22. I. GRENTHE et al., *Chemical Thermodynamics of Uranium*, H. WANNER and I. FOREST, Eds., OECD/NEA, North-Holland Elsevier Science Publishers B.V., Amsterdam, The Netherlands (1992).

23. R. J. SILVA, "Mechanisms for the Retardation of Uranium (VI) Migration," *Proc. European Materials Research Society*, Strasbourg, France, November 5–8, 1991 (Oct. 1991).

24. G. R. CHOPPIN and J. N. MATHUR, "Hydrolysis of Actinyl(VI) Cations," *Radiochim. Acta*, **52/53**, 25 (1991).

25. P. DÍAZ AROCAS and B. GRAMBOW, "Solid-Liquid Phase Equilibria of U(VI) in NaCl-Brines," *Geochim. Cosmochim. Acta*, **62**, *2*, 245 (1998).

26. A. SANDINO and B. GRAMBOW, "Solubility Equilibria in the U(VI)-Ca-K-Cl-H_2O System: Transformation of Schoepite into Becquerelite and Compreignacite," *Radiochim. Acta*, **66/67**, 37 (1994).

27. S. N. NGUYEN, R. J. SILVA, H. C. WEED, and J. E. ANDREWS, "Standard Gibbs Free Energies for Formation at 30°C of Four Uranyl Silicates: Soddyite, Uranophane, Sodium Boltwoodite, and Sodium Weeksite," LLNL UCRL-JC-106032, Lawrence Livermore National Laboratory (1991).

28. *Solubilities of Inorganic Compounds, Vol. 3, Ternary and MultiComponent Systems of Inorganic Substances, Part I*, H. L. SILCOCK, Ed., Pergamon Press, Oxford, United Kingdom (1979).

29. "EQ3/6 Software Package for Geochemical Modeling. Version 8.0" [software produced under the designated unclassified subject area (DUSA) "Yucca"], Lawrence Livermore National Laboratory (1997).

30. TH. FANGHÄNEL, V. NECK, and J. I. KIM, "Thermodynamics of Neptunium(V) in Concentrated Salt Solutions: II. Ion Interaction (Pitzer) Parameters for Np(V) Hydrolysis Species and Carbonate Complexes," *Radiochim. Acta*, **69**, 169 (1995).

31. B. KIENZLER and R. H. KÖSTER, "Experimental and Theoretical Investigations of Corrosion Mechanisms in Cemented Waste Forms," *Nucl. Technol.*, **71**, *3*, 590 (1985).

Bernhard Kienzler (MS, nuclear physics, 1974, and PhD, biological and geological sciences, 1976, Technical University Karlsruhe, Germany) has worked since 1977 at Forschungszentrum Karlsruhe (FZK), Institut für Nukleare Entsorgungstechnik. He is working in the fields of development and application of coupled speciation/transport codes, databases, scenario analyses, and performance assessment of radioactive waste disposal.

Peter Vejmelka (MS, chemistry, and PhD, chemistry, 1977, Rheinisch-Westfälische Technische Hochschule, Aachen, Germany) has worked since 1977 at FZK, Institut für Nukleare Entsorgungstechnik in the field of conditioning, characterization, and disposal of low- and intermediate-level radioactive wastes. His actual work covers experiments on sorption and migration of long-lived radionuclides in the near and far field of underground geologic disposals.

Horst-Jürgen Herbert (MS, geology, University of Bucharest, Romania, 1973; PhD, mineralogy and geochemistry, University of Tübingen, Germany, 1977) is an associate professor of geochemistry at the University of Kiel, Germany, starting in 1996. He is head of the Geochemistry Department of the Gesellschaft für Anlagen- und Reaktorsicherheit in Braunschweig, Germany. He is working

Downloaded by [the LANL Research Library] at 15:19 16 November 2017

in the area of underground disposal of radioactive and hazardous wastes. His background includes solution geochemistry and geochemical modeling.

Herbert Meyer (engineering degree, specialist in physical technology, University of Lübeck, Germany, 1980) beginning in 1980 was a scientific and technical collaborator at GSF-Forschungszentrum für Umwelt und Gesundheit, Forschungsbergwerk Asse. He is the head of the Department of Radiation Protection, a post he has held since 1989.

Corinna Altenhein-Haese (MS, mineralogy, 1988, and PhD, radiochemistry, 1996, Freie Universität Berlin, Germany) has been working since 1982 on various Commission of the European Communities projects on barrier performance of cement and concretes. Her background includes investigations into adsorption and migration in brines.

Downloaded by [the LANL Research Library] at 15:19 16 November 2017